

THE RLBL NEWSLETTER

Regional Laser and Biomedical Technology Laboratories
NIH/University of Pennsylvania

Robin M. Hochstrasser
Director

Thomas Troxler
Head of Laser Operations

NUMBER 23 MAY 2000

LOCAL NEWS:

There were significant changes in staffing at the RLBL since our last Newsletter was published. Charles M. Phillips, our long time Head of Laser Operations, has taken a position at Metrologic Instruments Inc., and Yiwei Jia, our single molecule spectroscopy guru, has taken a position at Olympus America Inc. We wish both Charles and Yiwei the best for their future endeavors.

Our two new staff members are Dr. Thomas Troxler and Dr. Erwen Mei. Thomas Troxler graduated Ph.D. from the University of Bern (Switzerland) in the group of Prof. S. Leutwyler. He was a postdoctoral associate at the chemistry department of the University of Pennsylvania and a visiting scientist at the Marshall Laboratories of DuPont de Nemours in Philadelphia. Tom will be doing research on conformational dynamics using photolysis and T-jump methods. Erwen Mei received his Ph.D. from Wuhan University (China) working in the microscopy group of Prof. Yun'e Zeng. Afterwards he spent one year in the National Agro-Environmental Institute as a Science and Technology Fellow of Japan and three years on single molecule research as postdoctoral associate at Kansas State University. Erwen will be doing single molecule experiments.

The RLBL continues its efforts to develop new laser methods and instrumentation for biomedical research. There were a number of exciting new discoveries arising from both our core and collaborative projects.

A principal focus of our core research program remains the development and application of two-dimensional IR spectroscopy, which are infrared analogues of NMR. We got a lot of attention with our latest results using heterodyned photon echo spectroscopy and spectrally resolved three pulse IR photon

echoes to investigate the amide I region and other transitions of small model peptides. The small number of C=O stretch modes allows for the measurement of the position and intensity of cross peaks in the multidimensional spectra, and to correlate these with structure. This subject forms the topic of the feature article by Asplund, Zanni and Hochstrasser of this Newsletter.

In the emerging area of terahertz (THz) spectroscopy, a new source of powerful THz and far-IR radiation was recently developed which employed a new four wave rectification (FWR) method. In the process of FWR, ultra-fast pulses with frequencies ω_0 and $2\omega_0$ interact, and the rectified component of the third order polarization radiates at frequencies on the order of 10^{12} Hz. These THz pulses were observed in ambient air, N₂ and Ar, and their peak field strength are more than sufficient in order to be used as a laboratory THz source.

There are also a number of exciting single molecule experiments underway at the RLBL. Most recently we reported single molecule measurements on the folding and unfolding conformational equilibrium distributions and dynamics of a disulfide cross-linked version of the two-stranded coiled-coil form of GCN-4 peptide in aqueous solution. End-to-end distance distributions have been characterized using fluorescent resonant energy transfer confocal microscopy. Correlation methods were used to investigate the folding dynamics of the peptide.

I would like to mention that we have updated our home-page on the World Wide Web (rlbl.chem.upenn.edu) in order to facilitate the efficient exchange of new and exciting information surrounding the Facility. If you have any comments about our home-page or any thought of becoming a user of the Facility, please send an email to my attention.

Thomas Troxler
ttroxler@mail.sas.upenn.edu

FEATURE ARTICLE

Vibrational Analogues of NMR: Two Dimensional Infrared Spectroscopy of Peptides (1)

M. C. Asplund, M. T. Zanni and
R. M. Hochstrasser
RLBL Laser Resource
University of Pennsylvania
Philadelphia, PA 19104-6323

Introduction

Exciting new experiments at RLBL have demonstrated that the idea of using multidimensional infrared (IR) spectroscopy to obtain molecular structures with sufficient time resolution to resolve barrier crossing processes and conformational dynamics, now appears to have exceptional promise (1-5). Important applications include conformational dynamics of molecules, peptides and perhaps small proteins in solutions. Such optimizations of vibrational spectroscopy require the ability to control the responses of particular vibrational transitions depending on their coupling to one another. In magnetic resonance the disentangling of complex spectra is accomplished by multiple pulse sequences that manipulate the spin coherences and populations. Therefore in IR spectroscopy multiple IR pulses having well defined spectral bandwidth, phase and amplitude will be required. Vibrational spectra could then be spread into a number of dimensions and the coupling between modes at different spatial locations within the molecule could be determined. Thus our strategy has been to regard the peptide or small protein as a network of coupled vibrators. The couplings between the separated excitations of this network are obtained

from multiple pulse IR experiments and then used to find three dimensional structures based on knowledge of vibrational dynamics, chemical connectability and the inter-mode potential functions. The successful implementation of such procedures will result in a significant advance in our ability to observe the time evolution of structural changes and of the couplings between different pieces of macromolecules.

We use three weak, phase controlled IR pulses to obtain the appropriate response of the molecules to the IR fields. To provide optimal spectral resolution by eliminating the inhomogeneous broadening in the infrared spectrum, we use the photon echo method. Both two-pulse (6) and three-pulse IR photon echoes (7) of vibrations have been studied previously, but in these reported echo experiments the generated third order field creates a signal on a square law detector, which is insensitive to the phase. Spectral resolution of the vibrational echo permits some phase relations to be obtained, but does not yield line-narrowed spectra. However the complete generated field amplitude and phase, free from any static inhomogeneous broadening, can be obtained in principle by means of infrared *heterodyne* echoes or spectral *interferometry* techniques.

The heterodyned echo method is used to examine responses from the single peptide vibrator, N-methylacetamide (NMA-d), and a dipeptide, acylproline. The Fourier transform of these echo signals along two experimentally controllable time axes yields the two dimensional IR spectra of the peptides from which structural and solvent effects and information about the phases of the contributions that give rise to the signals can be obtained. In addition, spectral

interferometry of the free decay of the echo signal is reported for acyl-proline. To the best of our knowledge these (1) are the first results that completely characterize the fields generated during the vibrational photon echo and that demonstrate all the weak signal infrared analogues of NMR using three pulses.

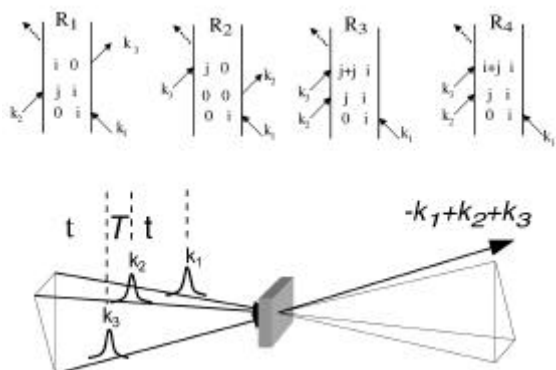


Figure 1: Pulse sequence and geometry used in the generation of the three pulse photon echo.

The infrared photon echo field

Three phase locked IR pulses, labeled 1, 2 and 3, and with wavevectors k_1 , k_2 and k_3 arrive at the sample with time intervals τ , between 1 and 2, and T , between 2 and 3. (see Figure 1) They create a polarization $P(t; \tau, T)$ in the sample for times t after the third pulse which in turn generates an electric field $E(t; \tau, T)$, the characterization of which is the aim of the current experiments. The IR photon echo is emitted in the phase matched direction $-k_1+k_2+k_3$, and for a system of vibrators it involves a number of intermediate vibrational coherences (8,9).

In an ideal heterodyne experiment, the signal field interferes on the detector with a short local oscillator field pulse and the heterodyne signal remaining after subtraction of the local oscillator intensity measures $S(\tau, t) = \text{Re}\{E(\tau, t)\}$. Both τ and t

can be scanned independently. In general the real generated field consists of sine and cosine parts (ie. it has a phase) which can be separately measured for a given τ from the real and imaginary parts of the Fourier transform of the signal along the t axis. The complex two dimensional IR spectrum is obtained from the Fourier transform of the $S(\tau, t)$, along τ and t , yielding frequency axes Ω_τ and Ω_t . A spectral interferogram is obtained when the signal plus local oscillator fields are dispersed in a monochromator, a procedure leading to a Fourier transform of the cross terms between the local oscillator and the signal fields on the square law detector. After subtraction of the local oscillator spectrum, the interferogram remains as the Fourier transform of $S(\tau, t)$ along the t -axis. Assuming that the monochromator is ideal this approach is more economical since it requires only a scan over τ (rather than t and τ) to obtain the two dimensional spectrum.

The simulated 2D IR spectrum $S(\Omega_\tau, \Omega_t)$ for a single oscillator is shown in Figure 2a. This spectrum has peaks, at $\{\Omega_\tau, \Omega_t\} = \{\omega, \omega\}$ and $\{\omega, \omega - \Delta_i\}$ where Δ_i is the anharmonicity of the i^{th} peptide mode with fundamental frequency ω . When the system consists of two or more vibrators, as in Figure 2b, there arise two types of peaks. The peaks on the diagonal, at $\{\omega, \omega\}$ and $\{\omega, \omega - \Delta_i\}$ represent single oscillator spectra. Other peaks occur at points $\{\omega, \omega\}$ and $\{\omega, \omega - \Delta_{ij}\}$ ($i \neq j$) which are in the cross peak region. The frequency and intensity of these cross peaks are related to the size of the couplings between the oscillators in given geometric configurations, which are in turn related to the spatial locations and relative orientations of the vibrators composing the network, and hence to the molecular structures that exist on the time scale of the measurement.

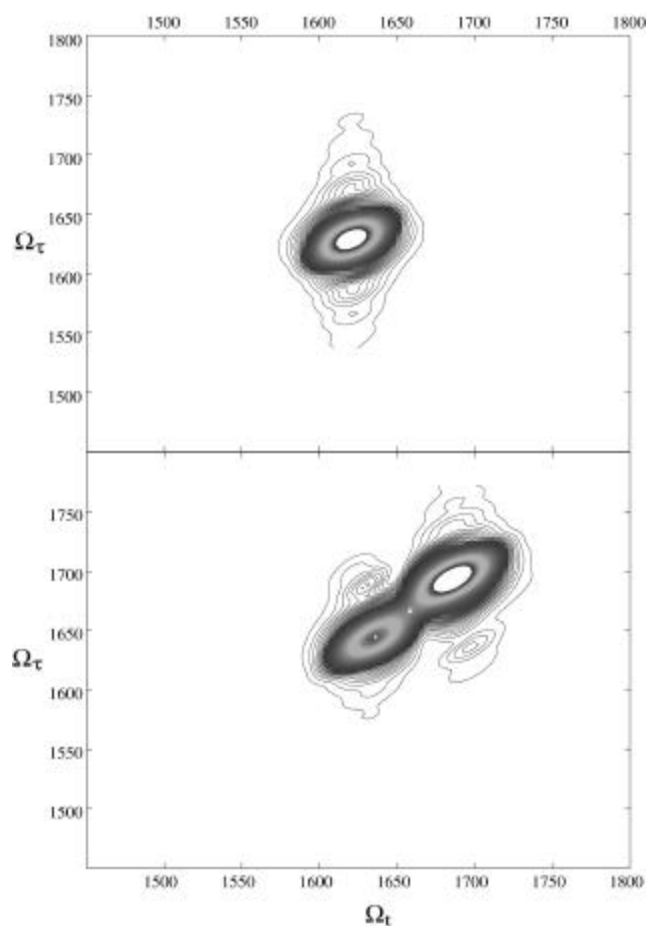


Figure 2: Simulations of absolute values of 2D-IR spectra, with a dephasing time of 900 fs, static inhomogeneous broadening of 9.5 cm^{-1} , and an anharmonicity of 16 cm^{-1} . (a) The 2D-IR spectrum for a single oscillator such as NMA-d, showing a single diagonal peak. (b) The 2D-IR spectrum for two oscillators, with a coupling of 5 cm^{-1} .

Instrumental development

The experiments need femtosecond infrared pulses (120 fs duration, $1 \mu\text{J}$ energy, 1 kHz repetition rate, 150 cm^{-1} bandwidth, 1600 cm^{-1} center frequency) which were generated by standard OPA and difference mixing methods developed at RLBL in the past few years. Three excitation pulses ($\sim 300 \text{ nJ}$ each), k_1 , k_2 and k_3 , and a fourth local

oscillator pulse ($\sim 30 \text{ nJ}$) are required. The timing of each of the pulses with respect to the k_2 pulse could be varied. The signal $S(\tau, t)$ contains oscillations at the frequencies of the vibrators, which are around 1600 cm^{-1} , and so have a period of ca. 20 fs. The generated echo emitted in the $-k_1 + k_2 + k_3$ direction (see Figure 1) was combined with the local oscillator field at a calcium fluoride beam splitter then the sum of the two collinear fields was focused onto the slits of a monochromator. Heterodyne echo signals were measured by placing a single channel MCT detector at the exit slits of the monochromator set to zero diffraction order, so that it reflects all frequencies onto the detector. For spectral interferometry these fields were dispersed on to an array detector.

Multiple pulse coherent infrared signals

Figure 3 shows $S(\tau, t)$ for NMA-d as a function of t , for several values of time (the time T was set equal to zero). The signal shows oscillations with a period of 20 fs, corresponding to the vibrational frequency of 1620 cm^{-1} . The Fourier transform of this signal gives the frequency spectrum of the emitted field (see Figure 3b) which shows a peak at 1620 cm^{-1} , the frequency of the amide stretch, and the width of this peak is insensitive to the time τ .

When the time variable τ is varied at fixed t_{LO} , an oscillatory signal is also generated. The complete two-time signal involves scanning over all τ for each possible value of t_{LO} . The Fourier transform, in both time dimensions, of this two-time signal is the complex two-dimensional frequency spectrum (the 2D-IR spectrum). The absolute value of the 2D-IR spectrum for NMA-d is shown in Figure 4a. NMA-d has only one oscillation

in this region of the spectrum, and so we see only one resonance in the 2D-IR spectrum.

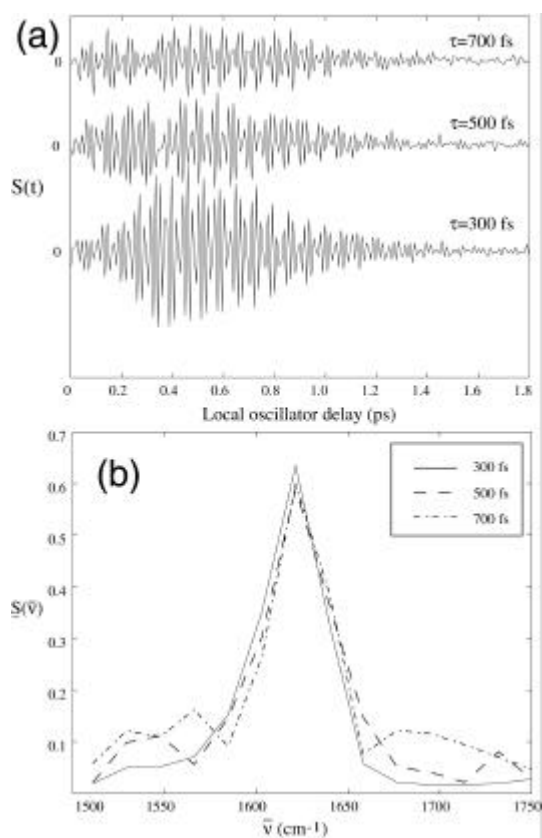


Figure 3: Heterodyne photon echo signals $S(\tau, T)$ for NMA-d in D_2O at several values of time t as a function of the time $t = t_{LO}$. (a) Time dependant interferogram of the echo signal, and (b) Fourier transforms along the τ axis showing the spectra of the signal.

Figure 4b shows the real part of the 2D-IR spectrum, corresponding to the real part of the dielectric susceptibility, we see that the $\nu=0 \rightarrow \nu-1$ and $\nu=1 \rightarrow \nu-2$ portions of the spectrum are separated because they have a different sign. Thus we see two peaks with opposite sign in the Ω_t direction, but only a single peak in the Ω_τ direction. (These data can also be examined by plotting the Wigner distribution (10) of the time dependentsignal which very clearly demonstrates the time dependent frequency shifts in the echo signal fields.)

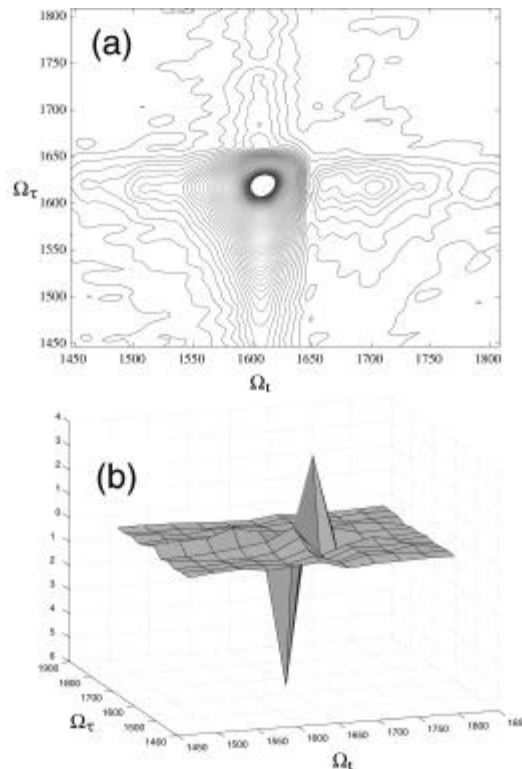


Figure 4: 2D-IR spectra for NMA-d in D_2O . (a) The absolute value of the 2D-IR spectrum, showing a single peak in both frequency dimensions. The asymmetry in the signal (cf. simulation of Figure 2) is sensitive to the choice of the center frequency of the laser pulses in relation to the resonances. (b) The real part of the 2D-IR spectrum, showing the fundamental and anharmonically shifted peaks, which have opposite signs.

These same experiments have been performed on systems with more than one amide unit. Figure 5 shows the heterodyne echo signal for the acylproline dipeptide in chloroform. Here again there is an oscillation with a period of 20 fs, and also a second lobe which appears about 1 ps after the first one. This is due to the interference between the two oscillations at 1610 cm⁻¹ and 1645 cm⁻¹. When this signal is Fourier transformed across the local oscillator delay, we obtain the spectra in Figure 5b, which show the signals from both of the

amide oscillators and their decay as a function of τ . When the data are collected as a function of both of the delays, t and τ , and then Fourier transformed along both time axes, the complex 2D-IR spectra for the acyl-proline are obtained.

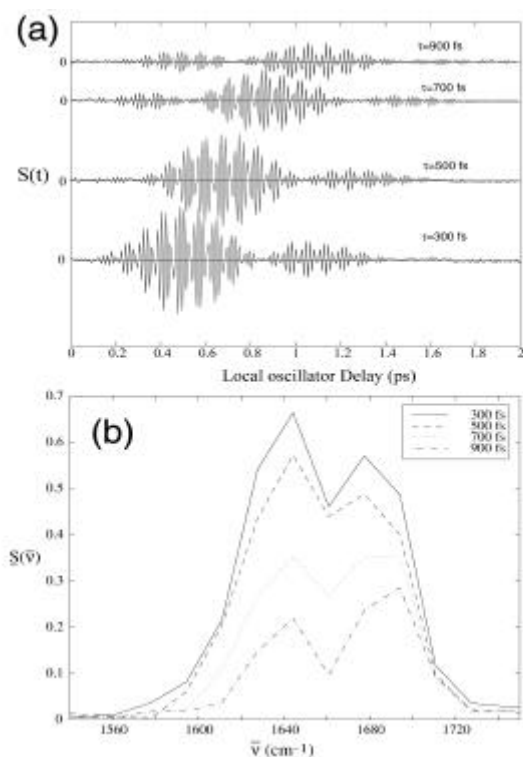


Figure 5: Heterodyne photon echo signal for acyl-proline in chloroform at several values of the time τ as a function of time t . (a) Time dependent echo signal and (b) the Fourier transforms showing the spectra of the echo signal.

Figure 6 shows the absolute value of these spectra for acyl-proline in D_2O and in chloroform. The spectra in both solvents show diagonal peaks at the frequencies of the oscillators. The 2D spectrum in chloroform also shows peaks off of the diagonal, in the spectral region where cross peaks are expected as described above. No off diagonal peaks were seen in the 2D-IR data of acyl-proline in D_2O .

The origin of the 2D IR spectrum

The origin of the 2D-IR spectrum is exemplified by the case of two vibrators a and b , separated in frequency by more than their coupling. Initially pulse 1 excites the vibrational coherent superpositions $0-a$ and $0-b$, which evolve for time τ . In the second step pulses 2 and 3, with $T=0$, transfer these coherences into their conjugates, $a-0$ or $b-0$, or into superpositions of $v=1$ and $v=2$ states. If the second step generates the $0-a$ or $0-b$ coherence then the same oscillations will occur along the τ and t axes and therefore the two dimensional spectra, along Ω_τ and Ω_t , will be diagonal. If, after initial excitation of the $0-a$ coherence, the next step produces the mixed mode (combination band) an a -peak will appear in Ω_τ and a b -peak in Ω_t . These *cross peaks* will only be manifest if the a and b modes are coupled in some way, and the 2D-IR spectrum provides a quantitative measure of this coupling.

The simplest example of these heterodyned spectra is a molecule that has only one mode (say, a) in the spectral region of interest. The system always responds with a frequency of ω_a during the time τ , and with frequencies of either ω_a or $\omega_a - \Delta_a$ during the time t . Therefore, the two dimensional Fourier transform of the total signal will have a single peak in the Ω_τ dimension, from the ω_a term, but will have two peaks in the Ω_t dimension, separated by the anharmonicity Δ_a . In the case of NMA-d the two peaks are only visible in the real part of the spectrum (see below) but not in the absolute value of the spectrum. Figure 4a shows the absolute value of the 2D-IR spectrum of NMA-d. The anharmonicity of 16 cm^{-1} is not resolved and the spectrum shows a single peak along the Ω_t axis. Nevertheless the very existence of this 3rd order echo signal

depends on the presence of anharmonicity.

Quantum mechanics predicts that the fields at ω_a and $\omega_a - \Delta_a$ should have opposite signs. In a heterodyne measurement, the electric field is measured directly, and so this sign information can be obtained. The double Fourier transform of $S(\tau, t)$ is related to the complex susceptibility, the real part of which is a 2D spectrum $\text{Re}\{S(\Omega_\tau, \Omega_t)\}$ which exposes the signs of the contributions to the signal. Figure 4b shows the real part of the 2D-IR spectrum of NMA-d. The sign difference between the two peaks is apparent and assists in the spectral resolution. The two peaks for NMA-d in the Ω_t axis are clearly separated by the anharmonicity of 16 cm^{-1} (see Figure 4b) though the frequency resolution is inadequate to fully resolve them in a conventional spectrum.

For molecules with more than one amide group, the signal now contains contributions for each oscillator as well as from their coupling. In the case of zero coupling the signal is a sum of isolated vibrator signals, which lie along the diagonal of the 2D-IR spectrum. The 2D-IR spectrum for acyl-proline in D_2O shown in Figure 6a exhibits this behavior. The data show peaks on the diagonal, at 1620 and 1670 cm^{-1} , but no other signals. This result indicates that there is no coupling manifested between the two oscillators. In the case of non-zero coupling the 2D-IR spectrum should show off-diagonal peaks at $\{\omega_i, \omega_j\}$ and at $\{\omega_i, \omega_j - \Delta_{ij}\}$. These two peaks have opposite sign, so when the coupling is small, they will cancel in the real part of the 2D-IR spectrum. However, when the coupling is large enough, there will be two peaks, with opposite sign.

Thus we can tell by the frequency separation of the cross peaks the exact value of the coupling element. The

intensity of the cross peaks in the absolute value $|S(\Omega_\tau, \Omega_t)|$ of the 2D-IR spectrum also enables the measurement of the coupling between the peaks. The data for the acyl-proline molecule chloroform (see Figure 6b) shows off-

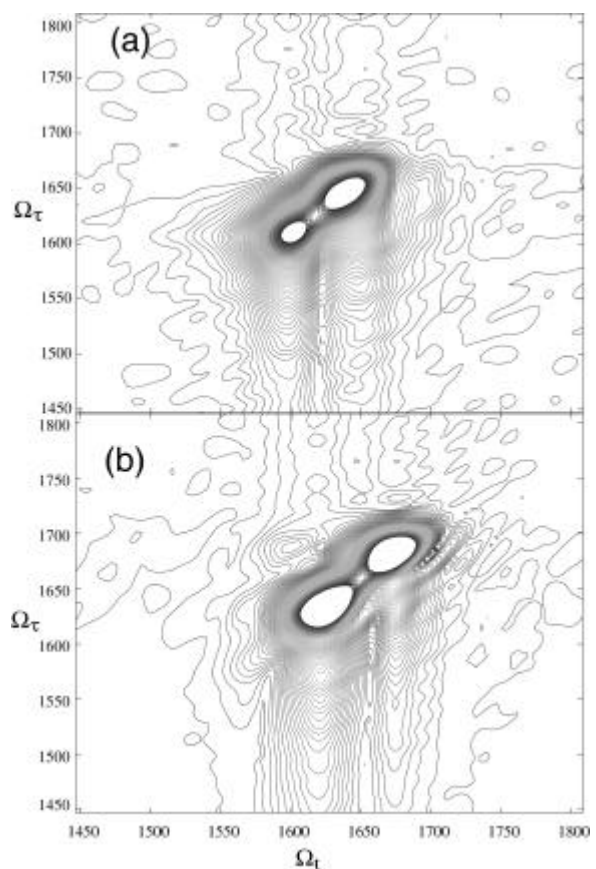


Figure 6: 2D-IR spectra of acyl-proline, in (a) D_2O , showing diagonal peaks at 1620 and 1670 cm^{-1} , and (b) in chloroform, which shows the same diagonal peaks, but also off diagonal peaks.

diagonal peaks in its absolute value 2D-IR spectrum, as expected for the signature of the coupling between the two oscillators. In CHCl_3 , acyl-proline has an internal hydrogen bond and adopts mainly an α structure whereas in D_2O the structure is less well defined (30). The electrostatic dipole-dipole coupling between amide units is calculated to be smaller for the α structure than for other structures so that the absence of 2D-IR coupling peaks in D_2O suggests that other coupling mechanisms, such as from mechanical

forces, may be contributing to the signal in the coupling region. The separation of the amide vibrational peaks of acyl-proline in D_2O is much larger (60 cm^{-1}) than the estimated coupling ($\sim 3\text{ cm}^{-1}$), a fact that can't be deduced from the linear IR spectrum.

An important feature of photon echo measurements is their spectral line narrowing capability. The generated field arises in general from an inhomogeneous distribution of vibrational frequencies representing the range of chemical environments and structures of the amide groups in the sample. The detected field therefore contains all the inhomogeneous component oscillations. It turns out that the effect of the inhomogeneous distribution of frequencies only shows up on the time axis (τ -t). As a consequence when the double Fourier transform is performed, the resulting 2D-IR spectrum is broadened by this distribution only along the axis $\Omega_\tau = \Omega_t$ (the diagonal axis of the 2D-IR spectrum). Along the perpendicular (antidiagonal) axis, $\Omega_\tau = \text{const.} - \Omega_t$, the spectrum shows no inhomogeneous broadening and can be optimally resolved.

In the NMA-d 2D-IR spectrum, the signal has similar width in both diagonals, and so static inhomogeneous broadening is absent from this spectrum. As a result the echo field is not noticeably delayed as τ is increased (Figure 3a). In the spectrum of the acyl-proline, however, the diagonal peaks are have an elliptical shape, with their longest axis in the $\Omega_\tau = \Omega_t$ direction. Along this axis the full inhomogeneous width of the transition is displayed, while in the dimension perpendicular to this, the spectral line is narrowed. In this case the signal is a true echo that is progressively delayed as τ increases (see Figure 5a). This line narrowing capability is particularly important because in solution, where the amide band is in general

inhomogeneously broadened, which causes peaks in the spectrum to overlap.

The frequency fluctuations of a vibrator are dependent on its solvent environment. Thus each vibrator should have its own relaxation dynamics dependent on its spatial location, chemical and solvent environment. The spectra for acyl-proline shown in Figure 6b show the peak at 1640 cm^{-1} decays much faster with τ than the peak at 1680 cm^{-1} . Previous work has suggested that in non-polar solvent, an internal hydrogen bond forms between the N-terminus end, and the acyl CO group (30). The two amide groups are therefore in very different environments, this is clearly signaled by their different dephasing dynamics. Experiments of this type will contribute significantly to obtaining microscopic views of peptide conformational dynamics and spatial aspects of solvent effects.

A related technique to the measurement of heterodyned echoes is the measurement of spectral interferometry of the echo signals. Here instead of measuring the frequency integrated signal at a number of local oscillator delay times, the frequency dependent signal at a single value of the local oscillator delay time is measured by dispersing the signal plus local oscillator fields in a monochromator. The signal after subtracting the intensity spectrum of the local oscillator is then the product of the echo spectrum, the local oscillator spectrum, and an oscillation whose frequency depends on the time delay of the local oscillator relative to the echo field. This interferometric signal is shown in Figure 7 for acyl-proline. Fourier analysis of the oscillatory part of the signal recovers the spectrum of the echo field as also shown in Figure 7. This spectrum shows peaks at 1610 and 1670

cm^{-1} , the two frequencies of the acyl-proline dipeptide.

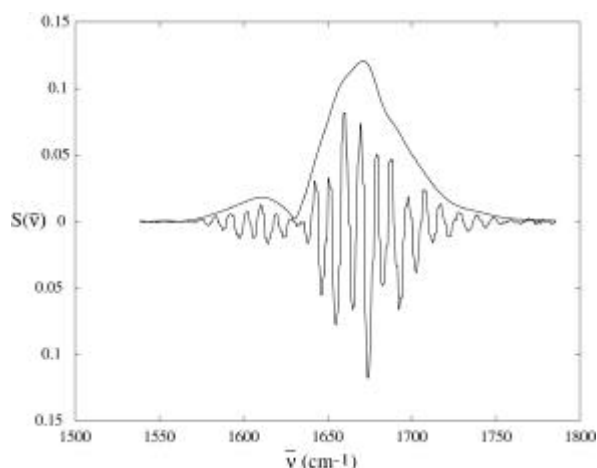


Figure 7: Spectral interferometry of the echo signal for acyl-proline in D_2O , with the local oscillator delayed 1.5 ps from the echo signal. Shown are both the measured interferometric signal and the processed signal, which represents the emitted electric field of the echo. This signal shows peaks at 1610 and 1670 cm^{-1} corresponding to the frequencies of the two amide units.

Summary and outlook

The use of phase controlled femtosecond infrared pulses enables the full measurement of two-dimensional vibrational spectra. These measurements are the direct infrared analogues of the multidimensional spectra measured in NMR experiments including multiple quantum transitions. They require phase matching and heterodyne mixing techniques to isolate and measure the electric field of vibrational photon echo signals as a function of three possible time variables. The Fourier transformed 2D-IR spectra provide information on couplings between modes and hence on peptide structures. The experimental time scale is less than a few picoseconds so there is no significant averaging of the signals by any structural dynamics slower

than this. Spectra that are free from inhomogeneous broadening were observed for acyl-proline. On the contrary, the amide transition of NMA-d showed no fixed inhomogeneous distribution of vibrational frequencies, so its inhomogeneous distribution is probably dynamic on the observation time scale. The measurement of the electric field of the echo enables separation of peaks in the echo spectrum on the basis of their signs, as shown in the 2-D spectrum of N-methyl acetamide. These methods show great promise for elucidating the *dynamics of structures in biology*.

Currently RLBL is engaged in a variety of experiments designed to broaden the scope of such experiments through variations of temperature and isotopic composition.

References:

1. M. C. Asplund, M. Zanni, and R. M. Hochstrasser, *Proc. Natl. Acad. Sci. USA* (in press).
2. P. Hamm, M. Lim, and R. M. Hochstrasser, *J. Phys. Chem. B* **102**, 6123 (1998).
3. P. Hamm, M. Lim, W. F. DeGrado, and R. M. Hochstrasser, *Proc. Natl. Acad. Sci. USA* **96**, 2036 (1999).
4. P. Hamm, M. Lim, W. F. DeGrado, and R. M. Hochstrasser, *J. Phys. Chem. A* **96**, 10049 (1999).
5. W. M. Zhang, V. Chernyak, and S. Mukamel, *J. Chem. Phys.* **110**, 5011 (1999).
6. A. Tokmakoff and M. D. Fayer, *J. Chem. Phys.* **103**, 2810 (1995).

7. P. Hamm, M. Lim, and R. M. Hochstrasser, *Phys. Rev. Lett.* **81**, 5326 (1998).
8. P. Hamm, M. Lim, W. F. DeGrado, and R. M. Hochstrasser, *J. Chem. Phys.* **112**, 1907-1916 (2000).
9. M. C. Asplund, M. Lim, and R. M. Hochstrasser, *Chem. Phys. Lett.*, in press.
10. L. Cohen, in *Time-Frequency analysis*, ed. A. V. Oppenheimer, A. V. Prentice Hall Inc., Madison (1995).

SUMMARY OF CURRENT TECHNOLOGICAL DEVELOPMENT AND RESEARCH AT RLBL

The main subjects under investigation at RLBL are shown below. If your research may be interfaced with any of these approaches we urge you to contact us. A fuller description of each of these categories can also be found on our Web site at <http://rlbl.chem.upenn.edu>.

e-mail: troxler@mail.sas.upenn.edu

- *Dynamics of photoactivatable proteins and other biological structures:* Methods are being developed to examine the responses of biological systems to light by pump/probe and nonlinear spectroscopic methods encompassing spectral regimes from the UV to the far IR and covering femtosecond to second timescales. Techniques include: single and multiple wavelength transient spectroscopy (UV/Vis, vibrational IR, Terahertz), photon

echos, two photon absorption and time-correlated single photon counting.

- *Methodologies to investigate protein folding and macromolecular conformational dynamics:* Detection and characterization of intermediate states in conformational dynamics and unfolding is another developing technology at RLBL. A laser-based temperature-jump apparatus was built for these investigations.

- *Investigations of single molecular assemblies using confocal and atomic force microscopes:* It is now possible to examine the properties of single molecules using fluorescence in association with confocal microscopy. The RLBL is coupling single molecule detection methods with mature time correlated photon counting technology, polarization scanning and pulsed laser experiments.

- *Energy transfer and fluorescence monitoring of biological dynamics:* Monitoring fluorescence lifetimes and anisotropies reveals details of protein dynamics. Techniques are being developed at the RLBL to monitor these properties of fluorescing species on the femtosecond to nanosecond timescale.

- *Development of time resolved far-IR (terahertz) probes for protein dynamical changes:* New powerful sources of THz and far-IR radiation are developed and used as laboratory THz source.

- *Two-dimensional infrared spectroscopy and infrared analogues of NMR:* Heterodyned photon echo spectroscopy and spectrally resolved three pulse IR photon echoes are employed to investigate the amide I region and other transitions of small model peptides.

A SELECTION OF RECENT COLLABORATIVE PUBLICATIONS

Distance distributions and correlation functions showing conformational dynamics in the folding of single GCN4 coiled-coil peptides by fluorescent energy transfer confocal microscopy. D. S. Talaga, W. L. Lau, Y.W. Jia, W. F. DeGrado and R. M. Hochstrasser, *Biophys. J.* **78**, 401A (2000).

Observation of folding dynamics of single GCN-4 peptides by fluorescence energy transfer confocal microscopy. Y. Jia, D. S. Talaga, L. Wei, H. S. M. Lu, W. F. DeGrado and R. M. Hochstrasser, *Biophys. J.* **76**, 10A (1999).

The dynamics of structural deformations of immobilized single light-harvesting complexes. M. A. Bopp, A. Sytnik, T.D. Howard, R. J. Cogdell, and R. M. Hochstrasser, *Proc. Natl. Acad. Sci. USA* **96**, 11271 (1999).

Folding dynamics of single GCN4 peptides by fluorescence resonance energy transfer confocal microscopy. Y. W. Jia, D. S. Talaga, W. L. Lau, H. S. M. Lu, W. F. DeGrado and R. M. Hochstrasser, *Chem. Phys.* **247**, 69 (1999).

Heme protein dynamics revealed by geminate nitric oxide recombination in mutants of iron and cobalt myoglobin, Y. Kholodenko, E. A. Gooding, Y. Dou, M. Ikeda-Saito, and R. M. Hochstrasser, *Biochemistry* **38**, 5918 (1999).

Femtosecond polarized pump-probe and stimulated emission spectroscopy of the isomerization reaction of rhodopsin, G. Haran, E. A. Morlino, J. Matthes, R. H. Callender, and R. M. Hochstrasser, *J. Phys. Chem. A* **103**, 2022 (1999).

Synthesis, spectroscopy, and ultrafast dynamics of soluble, conjugated porphyrin

arrays, K. Susumu, R. Kumble, R. M. Hochstrasser, M. J. Therien, *Abs. Pap. Amer. Chem. Soc.* **217**, 587-INOR (1999).

Peptidyl transferase center activity Observed in single ribosome. A. Sytnik, S. Vladmirov, Y. Jia, L. Li, B. S. Cooperman, and R. M. Hochstrasser, *J. Mol. Biol.* **285** 49 (1999).

Ultrafast studies of exciton dynamics in light harvesting dimers. D. C. Arnett, R. Kumble, R. W. Visschers, C. C. Moser, R. M. Hochstrasser, and N. F. Scherer, *SPIE: Laser Techniques for Condensed Phase and Biological Systems*, **3273**, 244 (1998).

Singlet and triplet excited states of emissive, conjugated bis(porphyrin) compounds probed by optical and EPR spectroscopic methods. S. Renee, M. H. B. Gray, H. T. Uyeda, R. C. Johnson, J. T. Hupp, P. J. Angiolillo, and M. J. Therien, *J. Am. Chem. Soc.* (in press).

A SELECTION OF RECENT CORE PUBLICATIONS

Femtosecond two-dimensional infrared spectroscopy of vibrations of peptides and molecules, N.-H. Ge, N. Milanovich, R. Kumble, and R. M. Hochstrasser, *Abstr. Pap. Amer. Phys. Soc.* [B15.015] (2000).

Multidimensional coherent infrared spectroscopy of small peptides, M. C. Asplund, J. M. Travins, F. A. Etzkorn, and R. M. Hochstrasser, *Abstr. Pap. Amer. Phys. Soc.* [B15.004] (2000).

Two-dimensional infrared spectra of peptide amide and N-H vibrations. R. M. Hochstrasser, P. Hamm, M. Lim, N. H. Ge, and W. F. DeGrado, *Biophys. J.* **78**, 13A (2000).

Pump/probe self heterodyned 2D spectroscopy of vibrational transitions of a small globular. P. Hamm, M. Lim, W. F. DeGrado and R. M. Hochstrasser, *J. Chem. Phys.* **112**, 1907 (2000).

Stimulated photon echoes from amide I vibrations. P. Hamm, M. Lim, W. F. DeGrado and R. M. Hochstrasser, *J. Chem. Phys. A* **103**, 10049 (1999).

Nonlinear 2-D IR spectroscopy of protein amide I vibrations. P. Hamm, M. Lim, and R. M. Hochstrasser, *Abstr. Pap. Am. Chem. Soc.* **U304** Part 2, (1999).

Terahertz-field-induced second-harmonic generation measurements of liquid dynamics, D. J. Cook, J. X. Chen, E. A. Morlino, and R. M. Hochstrasser, *Chem. Phys. Lett.* **309**, 221 (1999).

Coherence and adiabaticity in ultrafast electron transfer, K. Wynne and R. M. Hochstrasser, *Adv. Chem. Phys.* **107**, 263 (1999).

Effect of vibrational coherence on rotational dynamics in solution, S. Gnanakaran and R. M. Hochstrasser, *Int. J. Quantum Chem.* **72**, 451 (1999).

The two-dimensional IR nonlinear spectroscopy of a cyclic penta-peptide in relation to its three-dimensional structure, P. Hamm, M. Lim, W. F. DeGrado, and R. M. Hochstrasser, *Proc. Natl. Acad. Sci. USA* **96**, 2036 (1999).

The fifth-order contribution to the oscillations in photon echoes of anharmonic vibrators, P. Hamm, M. Lim, M. C. Asplund, and R. M. Hochstrasser, *Chem. Phys. Lett.* **301**, 167 (1999).

Energy transfer and localization: applications photosynthetic systems. S. Gnanakaran, G. Haran, R. Kumble, and R. M. Hochstrasser, in *Resonance Energy Transfer*, eds D. L. Andrews and A. A. Demidov, John Wiley and Sons, 308-365 (1999).

Chirped wavepacket dynamics of HgBr from photolysis of HgBr₂ in solution. M. Lim, M. F. Wolford, P. Hamm, and R. M. Hochstrasser, *Chem. Phys. Lett.* **290**, 355 (1998).

Vibrational Relaxation and dephasing of small molecules strongly interacting with water. P. Hamm, M. Lim, and R. M. Hochstrasser, in *Ultrafast Phenomena XI*: eds. T. Elsaesser, J. G. Fujimoto, D. Wiersma, and W. Zinth, Springer Verlag, Berlin-Heidelberg, p. 514-516 (1998).

Femtosecond dynamics, two-dimensional infrared spectroscopy and echoes of protein vibrations. R. M. Hochstrasser, P. Hamm, and M. Lim, in *Ultrafast Phenomena XI*: eds. T. Elsaesser, J. G. Fujimoto, D. Wiersma, and W. Zinth, Springer Verlag, Berlin-Heidelberg, p. 529-531 (1998).

Structure and dynamics of proteins and peptides: femtosecond two-dimensional infrared spectroscopy. P. Hamm and R. M. Hochstrasser, in *Ultrafast Infrared and Raman Spectroscopy*, ed. M. D. Fayer, Marcel Dekker, Inc. New York (in press).

Application for Use of the RLBL

Title:

Keywords (optional)

NIH Axis Numbers (optional)

Axis I

Axis II

Investigators (PI first)	Degree	Department	Institution	Address
1.				
2.				
3.				

NIH Support Sources Grant Number(s)	NIH Start/End Date (MM/DD/YY-MM/DD/YY)	Other Support Sources Agency and Grant Number(s)
1.		
2.		

Abstract: Describe briefly (200-250 words) the scientific goals and methods.

Logistics: Equipment to be supplied by applicant, needed from RLBL, and anticipated time.

Telephone Number:

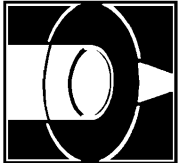
FAX Number:

E-Mail address (optional):

Date:

Mailing Address:

Send to: Professor R.M. Hochstrasser
Director, RLBL
Dept. of Chemistry
University of Pennsylvania
Philadelphia, PA 19104-6323



**THE REGIONAL LASER AND
BIOTECHNOLOGY LABORATORIES**
University of Pennsylvania
Philadelphia, PA 19104-6323

Non-Profit Organ.
U.S. Postage
Paid
Permit #2563
Phila., 4, PA